

Phase Diagram of One-Dimensional Extended Hubbard Model at Half Filling

M. Tsuchiizu and A. Furusaki

Yukawa Institute for Theoretical Physics, Kyoto University, Kyoto 606-8502, Japan

(Dated: October 24, 2018)

We reexamine the ground-state phase diagram of the one-dimensional half-filled Hubbard model with on-site and nearest-neighbor repulsive interactions. We calculate second-order corrections to coupling constants in the g -ology to show that the bond-charge-density-wave (BCDW) phase exists for weak couplings in between the charge density wave (CDW) and spin density wave (SDW) phases. We find that the umklapp scattering of parallel-spin electrons destabilizes the BCDW state and gives rise to a bicritical point where the CDW-BCDW and SDW-BCDW continuous-transition lines merge into the CDW-SDW first-order transition line.

PACS numbers: 71.10.Fd, 71.10.Hf, 71.10.Pm, 71.30.+h

Electronic correlations in solids have been a subject of intensive research over the years. Correlation effects have the strongest impact at commensurate band filling, where a system often undergoes a Mott transition. The one-dimensional (1D) extended Hubbard model (EHM) with the nearest-neighbor repulsion V , in addition to the on-site repulsion U , is a simple, but nontrivial model that exhibits rich phase structure [1]. The model has a long history of research, and considerable amount of knowledge has been accumulated. Much effort has been devoted to understanding its ground-state phase diagram at half filling. In the strong-coupling limit[1, 2, 3, 4] one can show that the model has two insulating phases, the spin-density-wave (SDW) phase and the charge-density-wave (CDW) phase, which are separated by a first-order transition line located at $U \simeq 2V$. In the weak-coupling limit the perturbative renormalization group (RG) analysis[1] concluded that there is a continuous phase transition between the CDW and SDW phases also at $U = 2V$. It was then considered that, as the coupling constants increase, the continuous-transition line changes into the first-order one at a tricritical point in the intermediate-coupling regime. This picture was supported by both numerical[3, 5, 6] and analytical[5, 7] studies and had been regarded as the complete phase diagram of the EHM at half filling.

Quite recently, however, Nakamura[8] found numerically that another phase exists between the CDW and SDW phases for weak couplings. The new phase is the bond-charge-density-wave (BCDW) phase in which the Peierls dimerization occurs spontaneously. He concluded that SDW-BCDW and BCDW-CDW transitions are continuous and that these two transition lines merge at a multicritical point into the first-order line separating the CDW and SDW phases [9]. His claim was confirmed by a recent extensive Monte Carlo calculation [10]. The appearance of a spontaneously dimerized phase in the EHM is surprising and calls for thorough theoretical study. So far the BCDW phase has been shown analytically to exist only in models with extra correlated-hopping interactions [11]. For the original EHM, however, the origin of

the BCDW phase and the nature of the associated phase transitions are not fully understood. In this Letter, we will provide theoretical argument for the existence of the BCDW phase by reformulating the weak-coupling theory to include higher-order terms. Using the bosonization technique, we derive a set of RG equations and discuss the critical properties of the phase transitions. We find that the umklapp scattering between electrons with parallel spins is responsible for the emergence of the bicritical point.

The Hamiltonian of the 1D EHM is

$$H = -t \sum_{j,\sigma} \left(c_{j,\sigma}^\dagger c_{j+1,\sigma} + \text{h.c.} \right) + U \sum_j n_{j,\uparrow} n_{j,\downarrow} + V \sum_j n_j n_{j+1}, \quad (1)$$

where $n_{j,\sigma} \equiv c_{j,\sigma}^\dagger c_{j,\sigma} - \frac{1}{2}$, $n_j \equiv n_{j,\uparrow} + n_{j,\downarrow}$, and $c_{j,\sigma}^\dagger$ denotes the creation operator of an electron at the j th site with spin σ . Following the previous studies on models with correlated-hopping interactions[11], we consider the CDW, SDW, BCDW and bond-spin-density-wave (BSDW) phases. They are characterized by the order parameters, $\mathcal{O}_{\text{CDW}} \equiv (-1)^j n_j$, $\mathcal{O}_{\text{SDW}} \equiv (-1)^j (n_{j,\uparrow} - n_{j,\downarrow})$, $\mathcal{O}_{\text{BCDW}} \equiv (-1)^j \sum_{\sigma} (c_{j,\sigma}^\dagger c_{j+1,\sigma} + \text{h.c.})$, and $\mathcal{O}_{\text{BSDW}} \equiv (-1)^j (c_{j,\uparrow}^\dagger c_{j+1,\uparrow} - c_{j,\downarrow}^\dagger c_{j+1,\downarrow} + \text{h.c.})$ [12].

We first focus on the weak-coupling limit $U, V \ll t$. The hopping t generates the energy band with dispersion $\varepsilon_k = -2t \cos k$. At half filling the Fermi points are at $k = \pm k_F = \pm\pi/2a$, where a is a lattice constant. Electrons experience two-particle scattering by the on-site and nearest-neighbor repulsions U and V . We follow the standard g -ology approach [1, 13] and parametrize the scattering matrix elements by the coupling constants g . In lowest order in U and V they are known to be $g_{1\parallel} = -2Va$, $g_{1\perp} = (U - 2V)a$, $g_{2\parallel} = 2Va$, $g_{2\perp} = (U + 2V)a$, $g_{3\parallel} = -2Va$, $g_{3\perp} = (U - 2V)a$, $g_{4\parallel} = 2Va$, $g_{4\perp} = (U + 2V)a$, where we have used the standard notation [1, 13]. Here we note that both $g_{1\perp}$ and $g_{3\perp}$ vanish at $U = 2V$, and this is the reason why the lowest-order calculation predicts the direct

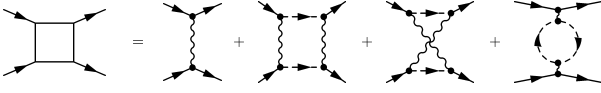


FIG. 1: Vertex diagrams. Solid lines denote the low-energy states and the dashed lines represent the high-energy states to be integrated out.

CDW-SDW transition at $U = 2V$. Hence, we need to go beyond the lowest order to see if the BCDW phase really exists. To this end, we adapt the two-step RG scheme used in Ref. [14]. (i) We separate the states into low-energy states ($||k| - k_F| < \Lambda$) and high-energy ones ($||k| - k_F| > \Lambda$) by introducing a momentum cutoff Λ , and integrate out high-energy states to obtain effective scattering matrix elements for low-energy states. (ii) We then derive one-loop RG equations for these matrix elements using the standard bosonization method. The diagrams for the effective couplings up to second order in U and V are shown in Fig. 1. The explicit calculation yields

$$g_{1\perp} = (U - 2V)a \left[1 - \frac{C_1}{4\pi t}(U - 2V) \right] - \frac{C_2}{\pi t} V^2 a, \quad (2)$$

$$g_{3\perp} = (U - 2V)a \left[1 + \frac{C_1}{4\pi t}(U + 6V) \right] + \frac{C_2}{\pi t} V^2 a, \quad (3)$$

where $C_1(\Lambda) \equiv 2 \ln[\cot(a\Lambda/2)] > 0$ and $C_2(\Lambda) \equiv 2 \cos(a\Lambda) > 0$. The weak dependences of C_i s on Λ allow us to set $\Lambda = \pi/4a$; different choices will only lead to small quantitative changes. We see that $g_{1\perp} < 0$ and $g_{3\perp} > 0$ at $U = 2V$ due to the C_2 term. This implies that a new phase different from the CDW and SDW can appear for $U \simeq 2V$, as we will show shortly. The zeros of $g_{1\perp}$ and $g_{3\perp}$ are shifted from $U = 2V$ due to the momentum dependence of the matrix element $2Va \cos(qa)$ for the virtual scattering of high-energy states ($q \neq 0, 2k_F$). There is no symmetry principle that enforces $g_{1\perp}$ and $g_{3\perp}$ to vanish simultaneously.

Having derived the effective scattering matrix elements for low-energy states, we now apply the bosonization method. The right-going and left-going electron fields $\psi_{\pm, \sigma}$ are written [1, 13]

$$\psi_{p, \sigma}(x) = \frac{\eta_\sigma}{\sqrt{2\pi a}} \exp[ipk_F x + ip \varphi_{p, \sigma}(x)], \quad (4)$$

where $\varphi_{p, \sigma}$ ($p = +/-$) are the chiral bosonic fields and $\{\eta_\sigma, \eta_{\sigma'}\} = 2\delta_{\sigma, \sigma'}$. The bosonic fields obey the commutation relations $[\varphi_{p, \sigma}(x), \varphi_{p, \sigma'}(x')] = ip\pi \text{sgn}(x - x') \delta_{\sigma, \sigma'}$ and $[\varphi_{+, \sigma}(x), \varphi_{-, \sigma'}(x')] = i\pi \delta_{\sigma, \sigma'}$. We define chiral charge fields, $\theta_p = (\varphi_{p, \uparrow} + \varphi_{p, \downarrow})/2$, and chiral spin fields, $\phi_p = (\varphi_{p, \uparrow} - \varphi_{p, \downarrow})/2$, to write the Hamiltonian density for low-energy states:

$$\mathcal{H} = \frac{1}{2\pi} \sum_{p=+, -} [v_\rho (\partial_x \theta_p)^2 + v_\sigma (\partial_x \phi_p)^2]$$

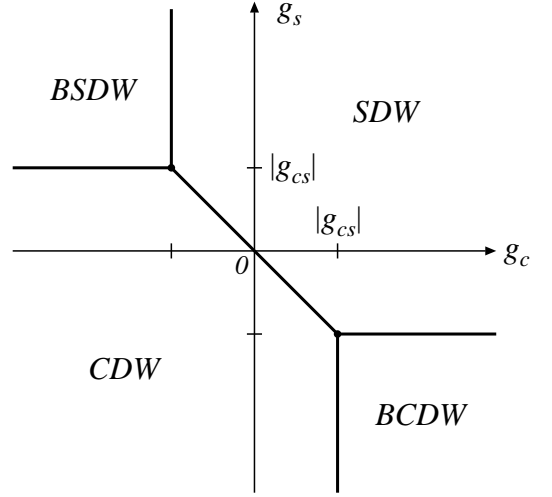


FIG. 2: Phase diagram obtained by minimizing the potential energy. Bicritical points are at $g_c = -g_s = \pm g_{cs}$.

$$\begin{aligned} & + \frac{g_\rho}{2\pi^2} (\partial_x \theta_+) (\partial_x \theta_-) - \frac{g_\sigma}{2\pi^2} (\partial_x \phi_+) (\partial_x \phi_-) \\ & - \frac{g_c}{2(\pi a)^2} \cos 2\theta + \frac{g_s}{2(\pi a)^2} \cos 2\phi \\ & - \frac{g_{cs}}{2(\pi a)^2} \cos 2\theta \cos 2\phi \\ & - \frac{g_{\rho s}}{2\pi^2} (\partial_x \theta_+) (\partial_x \theta_-) \cos 2\phi \\ & + \frac{g_{c\sigma}}{2\pi^2} (\partial_x \phi_+) (\partial_x \phi_-) \cos 2\theta \\ & + \frac{g_{\rho\sigma}}{2\pi^2} a^2 (\partial_x \theta_+) (\partial_x \theta_-) (\partial_x \phi_+) (\partial_x \phi_-), \quad (5) \end{aligned}$$

where $\theta = \theta_+ + \theta_-$, $\phi = \phi_+ + \phi_-$. The renormalized velocities are $v_\rho = 2ta + (g_{4\parallel} + g_{4\perp} - g_{1\parallel})/2\pi$ and $v_\sigma = 2ta + (g_{4\parallel} - g_{4\perp} - g_{1\parallel})/2\pi$. To simplify the notation, we have written $g_c = g_{3\perp}$, $g_s = g_{1\perp}$, and $g_{cs} = g_{3\parallel}$. The other coupling constants are given by $g_\rho = g_{2\perp} + g_{2\parallel} - g_{1\parallel}$, $g_\sigma = g_{2\perp} - g_{2\parallel} + g_{1\parallel}$, and $g_{\rho s} = g_{c\sigma} = g_{\rho\sigma} = -2Va$ to lowest order in V . The $g_{\rho s}$ ($g_{\rho\sigma}$) coupling comes from the backward scattering of electrons with opposite (parallel) spins, while the $g_{c\sigma}$ coupling is generated from the umklapp scattering of electrons with antiparallel spins. The SU(2) symmetry in the spin sector ensures $g_\sigma = g_s$, $g_{cs} = g_{c\sigma}$, and $g_{\rho s} = g_{\rho\sigma}$, and therefore it is important to retain the $g_{\rho\sigma}$ term.

In terms of the phase fields θ and ϕ the order parameters are written as

$$\mathcal{O}_{\text{SDW}}(x) \propto \cos \theta(x) \sin \phi(x), \quad (6)$$

$$\mathcal{O}_{\text{CDW}}(x) \propto \sin \theta(x) \cos \phi(x), \quad (7)$$

$$\mathcal{O}_{\text{BCDW}}(x) \propto \cos \theta(x) \cos \phi(x), \quad (8)$$

$$\mathcal{O}_{\text{BSDW}}(x) \propto \sin \theta(x) \sin \phi(x). \quad (9)$$

The phase diagram can be qualitatively understood via a quasi-classical analysis: we neglect spatial variations of the fields and focus on the potential, $V(\theta, \phi) =$

$-g_c \cos 2\theta + g_s \cos 2\phi - g_{cs} \cos 2\theta \cos 2\phi$, where $g_{cs} = g_{3\parallel} < 0$. The order parameters take maximum amplitudes when the fields θ and ϕ are pinned at the following potential minima: $(\theta, \phi) = (0, \pm\pi/2)$ in the SDW state, $(\pm\pi/2, 0)$ in the CDW state, $(0, 0)$ or $(\pi, 0)$ in the BCDW state, and $(\pi/2, \pm\pi/2)$ in the BSDW state (mod π). In these states the potential energy $V(\theta, \phi)$ becomes $V_{\text{SDW}} = -g_c - g_s - |g_{cs}|$, $V_{\text{CDW}} = g_c + g_s - |g_{cs}|$, $V_{\text{BCDW}} = -g_c + g_s + |g_{cs}|$ and $V_{\text{BSDW}} = g_c - g_s + |g_{cs}|$, respectively. Comparing these energies, we obtain the phase diagram in the g_c - g_s plane (Fig. 2). The direct CDW-SDW transition is first order because there is a potential barrier of height $\min(|g_{cs}|, 2|g_{cs}| - 2|g_c|)$ between the corresponding minima. The other boundaries located at $g_s = \pm|g_{cs}|$ and $g_c = \pm|g_{cs}|$ are continuous transitions, because the pinning potential for θ or ϕ vanishes when the other phase field is pinned. When $g_{cs} = 0$, the first-order CDW-SDW transition line collapses to a tetracritical point.

To obtain the ground-state phase diagram of the EHM, we need to include the renormalization of the coupling constants due to quantum fluctuations of the fields. A systematic analysis in the weak-coupling limit can be done by applying the perturbative RG method to \mathcal{H} (5). The SU(2) spin symmetry guarantees the relations $g_\sigma = g_s$, $g_{c\sigma} = g_{cs}$, and $g_{\rho\sigma} = g_{\rho s}$ to hold in the scaling procedure. The one-loop RG equations that describe changes of the coupling constants during the scaling of the short-distance cutoff ($a \rightarrow ae^{dl}$) are then given by

$$\frac{d}{dl}G_\rho = +2G_c^2 + G_{cs}^2 + G_s G_{\rho s}, \quad (10)$$

$$\frac{d}{dl}G_c = +2G_\rho G_c - G_s G_{cs} - G_{cs} G_{\rho s}, \quad (11)$$

$$\frac{d}{dl}G_s = -2G_s^2 - G_c G_{cs} - G_{cs}^2, \quad (12)$$

$$\begin{aligned} \frac{d}{dl}G_{cs} = & -2G_{cs} + 2G_\rho G_{cs} - 4G_s G_{cs} \\ & - 2G_c G_s - 2G_c G_{\rho s} - 4G_{cs} G_{\rho s}, \end{aligned} \quad (13)$$

$$\begin{aligned} \frac{d}{dl}G_{\rho s} = & -2G_{\rho s} + 2G_\rho G_s \\ & - 4G_c G_{cs} - 4G_{cs}^2 - 4G_s G_{\rho s}, \end{aligned} \quad (14)$$

where $G_\nu = g_\nu/(4\pi ta)$. From Eqs. (13) and (14) one finds that g_{cs} and $g_{\rho s}$ are irrelevant and renormalized towards zero for weak interactions. It is therefore natural to ignore g_{cs} and $g_{\rho s}$ first. With this approximation the Hamiltonian reduces to two decoupled sine-Gordon models, and it is easy to follow the RG flows of G_ρ , G_c , and G_s from Eqs. (10)–(12). Since $g_\rho = (U + 6V)a > 0$, G_c is relevant and grows at low energies. The coupling G_s is marginally relevant (irrelevant) for $g_s < 0$ ($g_s > 0$). The phase diagram of the EHM is obtained tentatively from Fig. 2 by setting $g_c = g_{3\perp}$ [Eq. (3)], $g_s = g_{1\perp}$ [Eq. (2)], and $g_{cs} = 0$. When U is sufficiently larger than $2V$ such that $g_c > 0$ and $g_s > 0$, we have the SDW phase. If U is

smaller than $2V$ ($g_c < 0$ and $g_s < 0$), then we have the CDW phase. Around the $U = 2V$ line we find the BCDW phase, where $g_{1\perp} < 0$ and $g_{3\perp} > 0$ due to the C_2 term. The BSDW phase does not exist in the EHM. The charge excitations are gapful except on the CDW-BCDW transition line where the relevant pinning potential vanishes. The spin excitations are gapless in the SDW phase and on the SDW-BCDW transition line and gapful otherwise. In the gapped phases the charge gap Δ_c and the spin gap Δ_s are given by $\Delta_c \simeq t|G_c|^{1/2G_\rho}$ and $\Delta_s \simeq t \exp(1/2G_s)$ for $|G_c| \ll 1$ and $0 < -G_s \ll 1$, respectively.

Next we examine effects of the parallel-spin umklapp scattering g_{cs} for $U \simeq 2V$. Let us assume $U - 2V = -C_2 V^2/\pi t + \mathcal{O}(V^3/t^2)$, i.e., $g_c \approx 0$ and $g_s < 0$. We are considering the situation very close to the CDW-BCDW transition. In this case the spin gap is formed first as the energy scale is lowered, and we can replace $\cos 2\phi$ with its average $\langle \cos 2\phi \rangle \simeq (\Delta_s/t)^2$ for energies below the spin gap. This means that the $\cos 2\theta$ potential that tries to pin the fluctuating θ field has the effective coupling

$$g_c^* = g_c + g_{cs} \langle \cos 2\phi \rangle. \quad (15)$$

The CDW-BCDW transition occurs when $g_c^* = 0$, i.e., $g_c = -g_{cs} \langle \cos 2\phi \rangle > 0$. The phase space of the BCDW state is reduced upon inclusion of the g_{cs} term. Note, however, that the CDW-BCDW boundary does not move across the $U = 2V$ line because $|g_{cs} \langle \cos 2\phi \rangle| \simeq 2Va \exp[-c(t/V)^2]$ is much smaller than the C_2 term for $V \ll t$, where c is a positive constant. A similar argument applies to the region near the SDW-BCDW transition. Suppose that $U - 2V = +C_2 V^2/\pi t + \mathcal{O}(V^3/t^2)$ ($g_s \approx 0$ and $g_c > 0$). In this case, as the energy scale is lowered, the charge gap opens first and the θ field is pinned at $\theta = 0$ (mod π). Below the charge-gap energy scale the ϕ field is subject to the pinning potential $g_s^* \cos 2\phi$ with

$$g_s^* = g_s - g_{cs} \langle \cos 2\theta \rangle, \quad (16)$$

where $\langle \cos 2\theta \rangle \simeq (\Delta_c/t)^{2(1-G_\rho)}$. The SDW-BCDW transition now happens at $g_s = g_{cs} \langle \cos 2\theta \rangle < 0$, and thus the SDW-BCDW transition line moves to increase the SDW phase. Again the phase boundary is not changed beyond the $U = 2V$ line as $|g_{cs} \langle \cos 2\theta \rangle| \simeq 2Va(c'V/t)^{\pi t/V}$ is much smaller than $V^2 a/t$, where c' is a constant of order 1. This completes our proof of the existence of the BCDW phase near the $U = 2V$ line in the weak-coupling limit.

For larger U and V , the g_{cs} coupling becomes less irrelevant, and the BCDW phase will eventually disappear. Since the cosine factor in Eqs. (15) and (16) can be considered as renormalization of g_{cs} , we conclude that the two continuous lines meet when the renormalized couplings satisfy the relation

$$G_c = -G_s = -G_{cs} \equiv G \quad (G > 0) \quad (17)$$

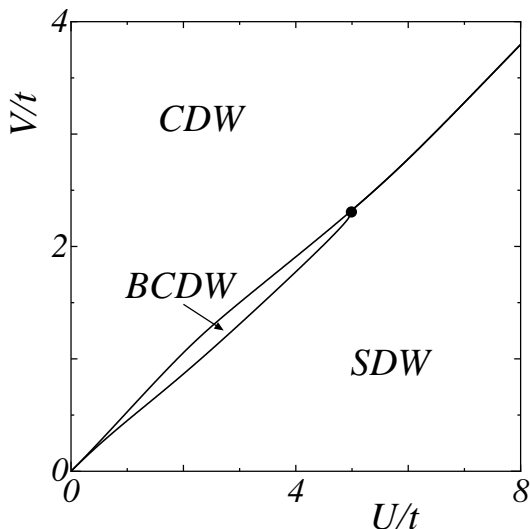


FIG. 3: Phase diagram of the half-filled extended Hubbard model. The bicritical point is at $(U_c, V_c) \simeq (5.0t, 2.3t)$.

in the low-energy limit. This is the condition for the bicritical point in the RG scheme. Note that the condition is not simply that the g_{cs} term becomes relevant, as previously assumed [5]. When Eq. (17) is satisfied, the effective potential takes a simple form $V(\theta, \phi) = -G(\cos 2\theta + \cos 2\phi - \cos 2\theta \cos 2\phi)$, which has an interesting feature that its potential minima are not isolated points but the crossing lines $\theta = \pi m$ or $\phi = \pi n$ (m, n : integer). On these lines either θ or ϕ becomes a free field; the theory has more freedom than a single free bosonic field, but less than two free bosonic fields. We thus expect that the theory of the bicritical point should have a central charge larger than 1 but smaller than 2. Detailed analysis of the critical theory is left for a future study.

We have numerically solved the scaling equations (10)-(14) to obtain the global phase diagram of the EHM. The phase is determined by looking at which of the couplings G_c , G_s , and G_{cs} becomes relevant. The idea is essentially the same as what we have discussed above. If $|G_c|$ grows with increasing l and reaches, say, 1 first among the 3 couplings, then we stop the integration and calculate $G_s^* = G_s - G_{cs}$. Since the charge fluctuations are suppressed below this energy scale, we are left with Eq. (12) where G_s replaced by G_s^* and $G_{cs} = 0$. We immediately see that a positive (negative) G_s^* leads to the SDW (BCDW) state. If $|G_s|$ becomes 1 first, then the sign of $G_c^* = G_c - G_{cs}$ determines the phase: the CDW (BCDW) state for $G_c^* < 0$ ($G_c^* > 0$). Finally, when $|G_{cs}|$ reaches 1 first, we stop the calculation and compare G_c and G_s . Since both charge and spin fluctuations are already suppressed by the $G_{cs} \cos 2\theta \cos 2\phi$ potential, we can deduce the phase from the quasi-classical argument. From Fig. 2 we see that we have the SDW state for $G_s > -G_c$ and the CDW state for $G_s < -G_c$. In the SDW state the pinning potential for the ϕ field is

marginally irrelevant, and therefore the spin sector becomes gapless. The phase diagram obtained in this way is shown in Fig. 3. For weak couplings the BCDW phase appears at $U \simeq 2V$, and the successive continuous transitions between the SDW, BCDW and CDW states occur as V/U increases. As U and V increase along the line $U = 2V$, the BCDW phase first expands and then shrinks up to the bicritical point $(U_c, V_c) \approx (5.0t, 2.3t)$ where the two continuous-transition lines meet. Beyond this point the BCDW phase disappears and we have the direct first-order transition between the CDW and the SDW phases. The phase diagram (Fig. 3) is similar to the one reported recently [8, 10]. The position of the phase boundaries in Fig. 3 is not reliable quantitatively however, as we have used the perturbative RG equations which are valid only in the weak-coupling regime.

In summary, we have studied the ground-state phase diagram of the 1D extended Hubbard model with repulsive interaction at half filling. We have shown analytically that the BCDW phase appears at $U \simeq 2V$ in the weak-interaction limit. We have also discussed the instability of the BCDW state and the emergence of the bicritical point due to the parallel-spin umklapp scattering.

M.T. thanks Y. Suzumura, H. Yoshioka, M. Sugiura, and, especially, E. Orignac for valuable discussions. This work was supported in part by Grant-in-Aid for Scientific Research on Priority Areas (A) from The Ministry of Education, Science, Sports and Culture (No. 12046238) and by Grant-in-Aid for Scientific Research (C) from Japan Society for the Promotion of Science (No. 10640341).

-
- [1] V. J. Emery, *Highly Conducting One-Dimensional Solids*, eds. J. Devreese, R. Evrard, and V. van Doren (Plenum, New York, 1979), p. 247.
 - [2] R. A. Bari, Phys. Rev. B **3**, 2662 (1971).
 - [3] J. E. Hirsch, Phys. Rev. Lett. **53**, 2327 (1984).
 - [4] P. G. J. van Dongen, Phys. Rev. B **49**, 7904 (1994).
 - [5] J. W. Cannon and E. Fradkin, Phys. Rev. B **41**, 9435 (1990); J. W. Cannon, R. T. Scalettar, and E. Fradkin, *ibid.* **44**, 5995 (1991).
 - [6] G. P. Zhang, Phys. Rev. B **56**, 9189 (1997).
 - [7] J. Voit, Phys. Rev. B **45**, 4027 (1992).
 - [8] M. Nakamura, J. Phys. Soc. Jpn. **68**, 3123 (1999); Phys. Rev. B **61**, 16377 (2000).
 - [9] Since the topology of the phase diagram is changed, the term ‘‘tricritical’’ is no longer appropriate for the multicritical point. Instead we will call it the bicritical point.
 - [10] P. Sengupta, A. W. Sandvik, and D. K. Campbell, cond-mat/0102141.
 - [11] G. I. Japaridze and A. P. Kampf, Phys. Rev. B **59**, 12822 (1999), and references cited therein.
 - [12] A. A. Nersisyan, Phys. Lett. A **153**, 49 (1991).
 - [13] J. Sólyom, Adv. Phys. **28**, 201 (1979).
 - [14] K. Penc and F. Mila, Phys. Rev. B **50**, 11429 (1994).